Plant Mol Biol
DOI 10.1007/s11103-012-9921-2

# A functional pectin methylesterase inhibitor protein (SolyPMEI) is expressed during tomato fruit ripening and interacts with PME-1

**Ida Barbara Reca · Vincenzo Lionetti · Laura Camardella · Rossana D'Avino · Thierry Giardina · Felice Cervone · Daniela Bellincampi**

Received: 30 September 2011 / Accepted: 3 May 2012


**Abstract** A pectin methylesterase inhibitor (SolyPMEI) from tomato has been identified and characterised by a functional genomics approach. SolyPMEI is a cell wall protein sharing high similarity with *Actinidia deliciosa* PMEI (AdPMEI), the best characterised inhibitor from kiwi. It typically affects the activity of plant pectin methylesterases (PMEs) and is inactive against a microbial PME. *SolyPMEI* transcripts were mainly expressed in flower, pollen and ripe fruit where the protein accumulated at breaker and turning stages of ripening. The expression of SolyPMEI correlated during ripening with that of PME-1, the major fruit specific PME isoform. The interaction of SolyPMEI with PME-1 was demonstrated in ripe fruit by gel filtration and by immunoaffinity chromatography. The analysis of the zonal distribution of PME activity and the co-localization of SolyPMEI with high esterified pectins suggest that SolyPMEI regulates the spatial patterning of distribution of esterified pectins in fruit.

**Keywords** Pectin methylesterification · Pectin methylesterase inhibitor · Fruit ripening · *Solanum lycopersicum*

Ida Barbara Reca and Vincenzo Lionetti contributed equally and are considered co-first authors.

**Electronic supplementary material** The online version of this article (doi:10.1007/s11103-012-9921-2) contains supplementary material, which is available to authorized users.

I. B. Reca · V. Lionetti · F. Cervone · D. Bellincampi (✉)
Dipartimento di Biologia e Biotecnologie "Charles Darwin", "Sapienza" Università di Roma, Piazzale Aldo Moro 5, 00185 Rome, Italy
e-mail: Daniela.bellincampi@uniroma1.it

*Present Address:*
I. B. Reca
Great Lakes Bioenergy Research Center, Michigan State University, East Lansing, MI, USA

L. Camardella · R. D'Avino
Institute of Protein Biochemistry, CNR, Via P. Castellino 111, 80131 Naples, Italy

T. Giardina
ISM2/BiosCiences UMR CNRS 7313, Faculté des Sciences, Aix-Marseille Université, service 342, 13397 Marseille Cedex 20, France

## Introduction

Pectin, the major component of the middle lamella and primary cell wall in dicotyledonous species, influences cell adhesion as well as the mechanical and textural characteristics of plant organs (Mohnen 2008). The structure of pectin undergoes changes during growth and development that include a de-esterification *in muro* of the methylesterified α-1,4-linked galacturonic acid backbone (HGA) by pectin methylesterases (PMEs) (E.C. 3.1.1.11). PMEs belong to Family 8 of carbohydrate esterases (http://www.cazy.org/fam/CE8.html) and are cell wall-associated enzymes that remove the methylesters from HGA to release methanol and protons in the apoplast. De-esterification affects the capability of HGA to form calcium-mediated cohesive egg-box structures that affect the gelling properties and porosity of the wall and makes HGA susceptible to the degradation by polygalacturonases (PGs) and pectate lyases (PLs) (Limberg et al. 2000; Raiola et al. 2011; Volpi et al. 2011). PMEs are widespread in plants and microorganisms and belong to large multigene families whose members display different roles as suggested by their diverse structures and expression patterns (Markovic

Published online: 19 May 2012

and Janecek 2001; Pelloux et al. 2007). Plant PMEs are involved in a number of reproductive and vegetative processes such as microsporogenesis and pollen tube growth (Wakeley et al. 1998; Futamura et al. 2000; Bosch et al. 2005), seed germination (Ren and Kermode 2000), root development (Pilling et al. 2004), leaf growth (Hasunuma et al. 2004), hypocotyl elongation (Bordenave and Goldberg 1993) and fruit ripening (Prasanna et al. 2007). The de-esterification of pectin and its metabolism play a role in fruit softening during ripening. In tomato transformed with an antisense chimeric PME gene, the reduction of PME activity influenced the pectin metabolism and increased the soluble solids content in ripening fruits (Tieman et al. 1992). The increase of PME as well of PG activity in tomato have been associated with fruit softening where a previous de-esterification by PME is required to make pectin susceptible to the hydrolytic de-polymerization by PG (Brummell and Harpster 2001; Wakabayashi et al. 2003; Prasanna et al. 2007). In addition to the temporal and organ-specific PME activity at different stages of growth and development, a spatial regulation at tissue and cellular level of PME activity is thought to be critical for the appearance of zonal changes of the pectin esterification (Steele et al. 1997; Kojima et al. 1991; McCartney et al. 2000; Blumer et al. 2000; Orfila et al. 2002; Vandevenne et al. 2009). At least eight PME isoforms have been identified in tomato (Markovic and Janecek 2004) two of them, termed PME-1 (P14280) and PME-2 (P09607), are specifically expressed in fruit (Markovic and Jörnvall 1986; Ray et al. 1988; Harriman et al. 1991; Hall et al. 1994) while, the ubiquitously expressed PMEU1 isoform (Q43143) is found in unripe fruit (Gaffe et al. 1997). PMEs have also a role in the plant response to a number of pathogens such as nematodes, viruses, fungi and bacteria (Dorokhov et al. 1999; Chen and Citovsky 2003; Hewezi et al. 2008; Raiola et al. 2011).

In addition to the transcriptional control, PME activity is regulated by endogenous inhibitor proteins (PMEIs) discovered in kiwi fruit (Balestrieri et al. 1990) and subsequently identified in pepper, broccoli, wheat (An et al. 2008; Peaucelle et al. 2008; Zhang et al. 2010; Hong et al. 2010) and Arabidopsis where 69 PMEI-related genes have been annotated (Raiola et al. 2004; Juge 2006; Jolie et al. 2010). Recent evidences demonstrate the role of PMEI in apical meristems development (Peaucelle et al. 2008), cell and organ size (Lionetti et al. 2007, 2010), cell growth acceleration (Pelletier et al. 2010) and pollen tube growth (Rockel et al. 2008; Zhang et al. 2010). PMEIs typically affect the activity of plant PMEs and do not inhibit bacterial and fungal enzymes (Di Matteo et al. 2005).

PMEIs are members of the multigene protein family PF04043 (http://pfam.sanger.ac.uk/) that also includes the invertase inhibitors (INHs); these share several structural properties with PMEIs but interact with unrelated enzymes (Scognamiglio et al. 2003). Here we provide the evidence that the genomic sequence SGN-U601352 from tomato (*Solanum lycopersicum* var. Moneymaker) encodes a functional PMEI (SolyPMEI) closely related to the kiwi inhibitor (AdPMEI; Camardella et al. 2000) and that a specific target of SolyPMEI in ripe fruit is PME-1 i.e. the main PME fruit isoform. Both SolyPMEI and PME-1 are co-expressed during fruit ripening and tissue localizations indicate that SolyPMEI inhibits PME activity and plays a role in the spatial distribution of esterified pectin in the fruit.

## Materials and methods

### Plant material

Tomato plants (*Solanum lycopersicum* cv Moneymaker) were grown in greenhouse. Fruits were harvested at the mature green stage (40 days post-anthesis), breaker stage (45 days post-anthesis), turning (50 days post-anthesis) and red ripe (55 days post-anthesis). *Nicotiana benthamiana* and Arabidopsis plants were grown as previously described (Ferrari et al. 2008).

### Gene identification and cloning of SolyPMEI

Nucleotide and amino acid sequences were identified on NCBI (http://www.ncbi.nlm.nih.gov/entrez/query.fcgi) and Solanaceae Genomic Network (SGN) (www.sgn.cornell.edu) databases. Signal peptide, putative cleavage site and putative glycosylation sites were predicted using SignalP 3.0, NetNGlyc 1.0 and DictyOGlyc (http://www.cbs.dtu.dk/index/shtml/). Alignment were performed with ClustalX and Bioedit (Hall 1999). Dendogram was inferred using the Neighbor-Joining method (Saitou and Nei 1987). The optimal tree with the sum of branch length = 403.2 is shown. All positions containing gaps and missing data were eliminated from the dataset. There were a total of 115 positions in the final dataset. Phylogenetic analyses were conducted using the MEGA 4.0 program (Tamura et al. 2007). The percentages of the replicate trees in which the associated sequences were clustered together in the bootstrap test (10,000 replicates) are shown next to the branches (Felsenstein 1985).

To isolate the full-length SolyPMEI cDNA, a 3′ RACE reactions was performed on total RNA extracted from tomato red fruit pericarp using:

a Gene-Specific Primer forward (GSP) (5′-GATTTGATAGATGAGATTTGCTCG-3′) and
a polyT reverse primer (5′-TTCTAGAATTCAGCGGCCGCTTTTTTTTTTTTTTTT-3′).

A nested PCR was carried out using the following forward primer:

5′-GCTCGAAAACAGATGTGAAG-3′

The PCR product was cloned using TOPO-TA cloning kit (Invitrogen) and several clones were sequenced. Full length *SolyPMEI* coding sequence was then amplified from tomato fruit cDNA using the following primers:

forward (5′-ATGGCACACTCATACAACTTCGCC-3′) and
reverse (5′-TCTAGATTACAAAAATCCAACAAGAACCAAAATAACATCG-3′), and amplicon was subcloned in TOPO-TA vector.

## Real time PCR

Different organs and fruits at the following stages of ripening: 40 (mature green), 45 (breaker), 50 (turning) and 55 days (red ripe) after anthesis were used. Tissues were frozen in liquid nitrogen, homogenized and total RNA was extracted using the Tri Reagent (Sigma). RNA was treated with Turbo-DNase I, and first strand cDNA was synthesized using ImProm-II reverse transcriptase (Promega). Real-time PCR analysis was performed using an iCycler (Biorad). cDNA (3 µl, corresponding to 120 ng of total RNA) was amplified in 30 µl of reaction mixture containing 1× Real Time SYBR Green JumpStart Taq ready Mix and 0.4 mM of each primer.

The synthesized *cDNA* were amplified using the following oligonucleotide primers:

*SolyPMEI* forward (5′-CATGTAATCTCGTTAGCACA-3′) and
reverse 5′AGAAGGTTCACGTATAGCAG-3′);
*PME-1* forward (5′-GCTTGCGTCTTTGACAACTCAGG-3′) and
reverse (5′-GTGCCACCACTGCATTCGCTAT-3′;
*PME2* forward (5′-CTTGCGTCTGTGACAACTCCAAA-3′) and
reverse (5′-CAATGTCCTTACCCGAACTCTCC-3′);
*PMEU1* forward (5′-CACGTCGAAGACCTGAAAACTCTAA-3′) and
reverse (5′-TCGCCGTTATCCTCTACTAACTTCC-3′);
*Actin 4* (*ACT4*) forward (5′-GGGATGATATGGAGAAGATA-3′) and reverse (5′-AGTACAGCCTGAATAGCAAC-3′).

The gene expression level was normalized to the expression of *ACT4* gene using a modified version of the Pfaffl method (Pfaffl 2001).

## Agrobacterium-mediated transformation of N. *benthamiana* leaves and preparation of intercellular washing fluid and total protein extracts

*SolyPMEI* coding sequence was subcloned in the pJD301 plasmid. The cassette, comprising the *35S* promoter of Cauliflower mosaic virus, the Ω leader of Tobacco mosaic virus, the *SolyPMEI* open reading frame, and the nopaline synthase 3′ sequence, was inserted into the HindIII/EcoRI site of the pBI121 vector. Construct was mobilized in *Agrobacterium tumefaciens* (strain GV3101) used to transiently transform *N. benthamiana* leaves as described (Reca et al. 2008). *A. tumefaciens* transformed with *35S::SolyPMEI* was injected in tobacco leaves at one side of the middle vein and the other half was transformed with *Agrobacterium tumefaciens* containing the empty pBI vector, as negative control. Intercellular washing fluids (IWFs) were collected by infiltration-centrifugation technique (Lohaus et al. 2001) from transiently transformed *N. benthamiana* leaves 48 h post agro-infiltration, as previously described (Lionetti et al. 2007) with some modifications. Leaves were vacuum-infiltrated with buffer containing 0.2 M NaCl, 20 mM NaOAc pH 4.7. Total protein extracts were prepared from tobacco leaves before and after IWF collection by homogenization in a blender at 4 °C in the buffer as above (1 ml/g of tissue). Homogenates were shaken for 10 min, centrifuged at 15,000*g* for 20 min at 4 °C and supernatants were collected. Glucose 6-phosphate dehydrogenase (G6PDH) activity was measured spectrophotometrically as previously described (Sicilia et al. 2005) and PME activity determined as described below.

## Agrobacterium-mediated transformation of Arabidopsis leaf epidermal cells and Confocal Microscopy

The *secGFP-SolyPMEI* plasmid was generated by inserting *SolyPMEI* cDNA sequence into GFP-containing vector psGFP5T (Di Sansebastiano et al. 1998) as a BglII/PstI fragment, excluding the region encoding the signal peptide. The restriction sites were introduced using the following primers:

forward (5′-CTTGATCGGTTCATCATACGCAGATCTTGATTTGAT-3′) and
reverse (5′-CACATGATGAAAGATCTGCAGATTACAAAAATCC-3′).

*SecGFP-SolyPMEI* was inserted as EcoRI/SacI fragment into the plant binary vector (Haseloff et al. 1997) and the final construct was checked by DNA sequencing (Primm, Milano, Italy). *SecGFP-SolyPMEI* construct was introduced into *Agrobacterium tumefaciens* (strain GV3101) and transiently expressed in leaves as previously

described (De Caroli et al. 2011). Observations were made 48 h after agroinfiltration using a Spinning-disk confocal microscope (CarvX; CrEST-Italy). The GFP was excited using 473 nm wavelength laser light and detected using a cooled charge-coupled device CCD camera (CoolSNAP HQ2, Photometrics, USA) through Semrock Brightline (USA) band-pass filters, respectively for GFP (495 nm edge dichroic, 520 nm/35 nm emitter). The CCD camera, Z-motor and Confocal head were controlled with Metamorph software (Molecular Devices, USA).

## Expression in *Pichia pastoris*

*SolyPMEI* gene was amplified by PCR from TOPO-SolyPMEI construct, using the following primers:

forward (5′-GAATTCGATTTGATAGATGAGATTTG CTC-3′) and
reverse (5′-TCTAGATAGAAGGTTCACGTATAGC ACGAG-3′).

The amplification products were isolated and cloned between the EcoRI and XbaI restriction sites into pPICZαA vector and used to transform *P. pastoris* strain X-33 according to the Pichia EasyComp™ transformation kit (Invitrogen).

Transformed *P. pastoris* cells were grown in flasks to saturation in BMGY medium at 28 °C under shaking at 250 rpm. After centrifugation at 10,000*g* the collected yeast cells were grown for 72 h in a modified BMMY medium (0.4 % (w/v) yeast extract, 0.6 % (w/v) tryptone, 100 mM potassium phosphate pH 6.0, 1.34 % (w/v) yeast nitrogen base (YNB), 0.4 g/ml biotin, 1 % (v/v) methanol). Methanol, to a final concentration of 0.5 % (v/v), was added every 24 h.

## Protein extraction, purification and analysis

After growth the Pichia culture was centrifuged at 10,000*g* for 15 min and the supernatants was treated with ammonium sulfate 85 % saturation and centrifuged at 10,000*g* at 4 °C. The precipitate was dissolved in 20 mM Na acetate pH 5, extensively dialyzed in the same buffer and loaded onto a DEAE column. The eluted proteins were collected, loaded onto a MonoS column (HR 10/10, Pharmacia) and eluted with a linear gradient ranging from 0 to 0.5 M NaCl in 20 mM NaOAC, pH 4.5 using an FPLC system (Pharmacia). The purity of the recombinant SolyPMEI was checked by SDS-PAGE and silver staining and fractions containing SolyPMEI were pooled and concentrated by ultrafiltration on Centricon 3 filters (Amicon).

The recombinant SolyPMEI (10 µg) was N-deglycosylated using 1,000 U of endoglycosidase H (New England BioLabs). The disulfide bridges arrangement was determined after alkylation of SolyPMEI with 4-vinylpyridine, before and after reduction with dithiothreitol, digestion with trypsin (Roche Applied Science) and HPLC analyses of obtained peptides were performed as described (Camardella et al. 2000).

Total proteins were extracted from tomato tissues by homogenization in a blender at 4 °C in a buffer (1 ml/g of tissue) containing 1 M NaCl, 20 mM NaOAc, pH 4.7. Homogenates were shaken for 10 min, centrifuged at 15,000 *g* for 20 min at 4 °C and supernatants were collected.

Gel filtration chromatography was performed on supernatants after protein precipitation with ammonium sulfate (85 %). The precipitate was suspended in 20 mM Na acetate pH 4.5, 250 mM NaCl and loaded onto a Superdex75 (HR10/30), eluted with the same buffer at a flow rate of 0.5 ml $min^{-1}$ and fractions of 0.5 ml were collected. SDS-PAGE and Western blot analysis were performed using anti-SolyPMEI antibodies purified as below described.

N-terminal amino acid sequencing of recombinant SolyPMEI, natural SolyPMEI and PME-1 from tomato was performed after SDS-PAGE and electro-transfer onto a polyvinylidene difluoride membrane as described previously (Matsudaira 1987). Automated repetitive Edman degradation was made on a model 494 Procise™ Protein Sequencer (Applied Biosystems Division).

MS/MS analysis of natural SolyPMEI from tomato was performed on proteins after SDS-PAGE separation and in-gel digestion using trypsin (Promega) as described (Shevchenko et al. 1996). An aliquot of the peptide mixture was treated with 0.2 mU of N-glycosidase A (Roche Applied Science) in 0.1 M citrate/phosphate buffer pH 5.0 at 37 °C for 22 h. Nano-HPLC–ESI–MS analysis was performed in information dependent acquisition (IDA) mode with a QStar-Elite (Applied Biosystems) triple quadrupole time-of-flight instrument equipped with a nano-ES ion source and online coupled to Ultimate-3000 HPLC system (Dionex). Peptide mixtures were purified and concentrated on PepMap C18 pre-column (300 µm × 5 mm, 5 µm, 100 Å, LCPackings) at 30 µl/min flow rate, and subsequently separated at flow rate 300 nl/min using a PepMap C18 column (75 µm × 15 cm, 3 µm, 100 Å, LCPackings). The peptide mixture was eluted using a linear gradient from 5 to 65 % of acetonitrile in 0.1 % formic acid, 0.025 % trifluoracetic acid. The eluate was directly injected into the nano-ES ion source. The two most abundant ions with multiple charges from 2 to 4 were selected for automated MS/MS acquisition. Nitrogen was used as collision gas. MS/MS peak lists were created by using Analyst QS 2.0 (Applied Biosystems) software. A local database containing the putative tomato PMEI sequence was created and utilized for data matching using the Mascot Server Version 2.2.04

search engine. The parameters used were the following: trypsin as enzyme, up to 2 missing cleavages allowed, carbamidomethylation as fixed modification of cysteine, oxidation of methionine and deamidation of asparagine as variable modifications.

### Immuno affinity chromatography

Rabbit polyclonal antibodies against the SolyPMEI expressed in *P. pastoris* generated by Primm were purified onto a CNBr-SolyPMEI affinity column in which recombinant SolyPMEI was previously covalently linked to CNBr activated Sepharose resin as previously described (Cervone et al. 1987). Antiserum was loaded onto the column, washed with ten volumes of PBS and the antibodies were eluted with 0.1 M glycine pH 2.0 and immediately neutralized.

To partially purify the natural SolyPMEI in complex with the enzyme, total proteins were isolated from red tomato fruits dialyzed against 10 mM PBS, loaded onto an anion exchange DEAE column and the protein fraction that did not bind to the column (i.e. flow though; FT) was collected. The proteins were loaded onto the immune-affinity column prepared using purified SolyPMEI antibodies covalently linked to CNBr-Sepharose. The column was washed with ten volumes of PBS containing 500 mM NaCl to remove nonspecific ionically interacting proteins and SolyPMEI eluted with 0.1 M Glycine pH 2.0 and immediately neutralized. No protein bands were retained by a blank CNBr-Sepharose column when tomato extracts were loaded under the same conditions.

### Protein modeling

Comparative modeling was performed on a Silicon Graphics O2 workstation, using Homology (Greer 1990) and MODELER (Sali and Blundell 1993) software programs in the InsightII molecular modeling system from Accelrys Inc. The molecular model of SolyPMEI in complex with tomato PME was built using the complex AdPMEI/tomato PME (PDB code 1XG2) as a structural template(Di Matteo et al. 2005). Sequence alignment of the proteins was submitted to MODELER (Accelrys.inc) for subsequent minimization. The protocol included careful refinement of the loop regions. A set of 6 models was generated. Analysis of the structural violations of the probability density function (PDF) was performed on each model structure. The $\phi$ and $\varphi$ angles of the residues were assessed from the Ramachandran plot obtained using the Swiss-PDB Viewer program.

### PME activity assays

The PME activity was determined by a coupled spectrophotometric enzyme assay based on methanol oxidation via alcohol oxidase (AO) and subsequent oxidation of formaldehyde by formaldehyde dehydrogenase (FDH) as previously described (Grsic-Rausch and Rausch 2004). The reaction mixture consisted of 894 µl 0.4 mM NAD in 50 mM phosphate buffer pH 7.5, 80 µl 2.5 % (w/v) 70–75 % esterified apple pectin (SIGMA 76282) in $H_2O$, 8 µl (0,35 U) FDH (from *P.putida*, F1879; Sigma) and 8 µl (1.0 U) AO (from *P.pastoris*, A2404; Sigma). PME from orange peel (SIGMA P0764), tomato red fruit crude extract, *Erwinia chrysantemi* (a gift from Danisco Innovation, Denmark) and SolyPMEI were utilized. Heat denatured (95° C, 5 min) PME or SolyPMEI were used as negative controls. SolyPMEI and PME (both in 10 µl aliquots) were pre-incubated for 15 min and then added to the reaction mixture. Reaction rate was recorded at 340 nm and PME activity was determined by measuring the rate of NADH formation per minute at 25 °C. One PME unit is defined as 1 µmol NADH formed per minute at pH 7.5 and 25 °C.

PME activity was localised in radial fruit sections using a substrate-gel assay as described (Blumer et al. 2000). In particular, medial radially sliced sections from tomato fruits were briefly dried on Whatman 3MM paper and subsequently blotted for 5 min on a 0.1 mm tick-gel consisting of 0.2 % apple pectin (75 % methylesterified; SIGMA 76282) cast on 1.5 % agarose. After blotting, the gel was stained with 0.1 % ruthenium red (w/v) for 10 min, followed by extensive washing with $H_2O$. PME activity resulted in a persistent dark red staining.

### Determination of the degree of pectin methylesterification

Tomato pericarp tissues (1 gr) were frozen in liquid nitrogen and the ground tissue was washed twice in 70 % ethanol, vortexed and pelleted by centrifugation at 10,000 *g* for 10 min. The pellet was suspended with a chloroform–methanol mixture (1:1 v/v). After centrifugation and evaporation of the solvent cell wall material was saponified and methanol, uronic acid contents and degree of methylesterification determined as previously reported (Lionetti et al. 2007).

### Immunoblot analysis and immune-tissue printing

To immunodetect SolyPMEI or PME-1/2, 10 and 3 µg, respectively, of total proteins isolated from tomato fruits at different stages of ripening were separated on SDS-PAGE and immunoblot analysis were performed using respectively, purified antiSolyPMEI antibodies (1:5,000 dilution) or monoclonal antibodies MA-TOM1-41B2 as described (Vandevenne et al. 2009). Immuno tissue printing was performed by pressing tomato tissues onto nitrocellulose membranes as previously indicated (Vandevenne et al.

2011) and SolyPMEI and methylesterified pectins detected using, respectively, purified rabbit antiSolyPMEI antibodies or rat monoclonal LM20 antibodies (1:200 dilution) specific for methylesterified homogalacturonan (Verhertbruggen et al. 2009). As negative controls the tissue-prints were incubated with the respective secondary antibodies conjugated with horseradish peroxidase without primary antibody.

## Results and discussion

### Identification, characterization and apoplastic localization of SolyPMEI

A search for Solanaceae genes encoding pectin methylesterase inhibitors in NCBI database (http://www.ncbi.nlm.nih.gov/blast/Blast.cgiand) and Sol genomic database (http://www.sgn.cornell.edu/) revealed a number of sequences exhibiting amino acid identities above 30 % with PMEI from kiwi (AdPMEI: P83326). A phylogenetic tree generated with the sequences encoding all characterized members of the INH/PMEI inhibitors PF04043 family identified three independent groups (Fig. 1). Group 1 includes the functional INHs and the recently characterised TaPMEI from wheat (Hong et al. 2010). Group 2, evolutionarily related to group 1, includes two functional PMEIs from *Actinidia deliciosa* (kiwi) fruit (Giovane et al. 1995; Hao et al. 2008), the two pollen specific PMEIs from *Arabidopsis thaliana* (Wolf et al. 2003; Raiola et al. 2004) and the deduced amino acid sequence of a cDNA fragment of *Solanum lycopersicum* cv TA496 isolated from red fruit pericarp (SGN-U601352), hereafter named *SolyPMEI*. Group 3 comprises CaPMEI1 from pepper (An et al. 2008), mainly expressed in stems and involved in biotic and abiotic stresses, the pollen specific BoPMEI from broccoli with a role in pollen tube growth (Zhang et al. 2010), the Arabidopsis PMEI3 expressed in apical meristems and affecting primordia formation (Peaucelle et al. 2008) and PMEI4 specifically expressed in Arabidopsis hypocotyls and root epidermal cells and thought to be involved in the regulation of growth acceleration (Pelletier et al. 2010). The distribution of PMEIs in different independent groups indicates the large diversity of the PMEI members either inside the same or among different plant species. This variability likely has a functional role and reflects the organ specific expression pattern as well as the need of specific interaction of given PMEIs and PME isoforms. Previous studies indicate five different tissue-specific expression clusters each of which containing defined PMEs and PMEIs in Arabidopsis (Wolf et al. 2009).

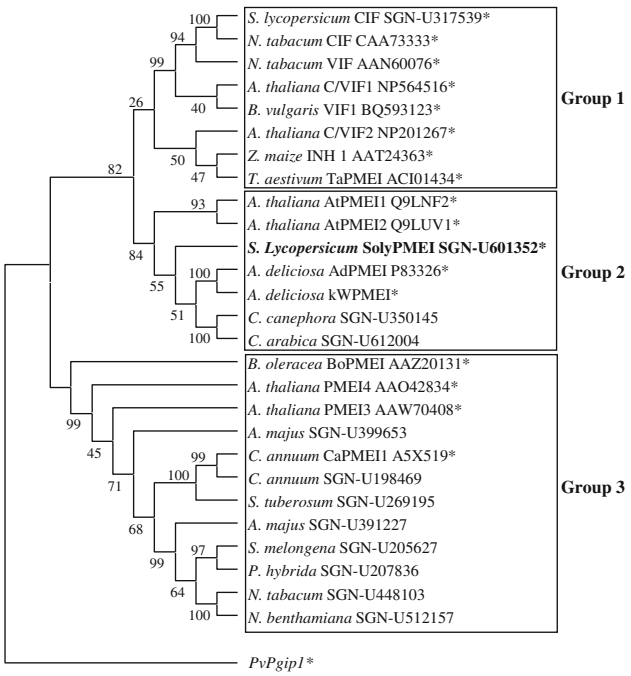


**Fig. 1** Evolutionary tree of 27 selected PMEI and INH members. The tree is based on alignment of mature protein sequences. Polygalacturonase inhibiting protein 1 from *Phaseolus vulgaris* (PvPgip1: P35334) was used as outgroup. The amino acid sequence of *A. deliciosa* kWPMEI was included as previously determined (Mei et al. 2007). *Asterisks* label functionally characterized inhibitors

The lacking 3′ portion of the *SolyPMEI* gene was determined by sequencing the cDNA obtained from red fruit of *S. lycopersicum* cv. Moneymaker, using the 3′-RACE technique. The nucleotide sequence of *SolyPMEI* gene is in agreement with the sequence of SGN-U601352 fragment, except for a difference in position 452(A → G) responsible for the amino acid modification Lys151 → Arg that may be due to allelic micro-heterogeneity between the different tomato cultivars used (Fig. S1). According to BAC sequencing data, the *SolyPMEI* gene is located in the third chromosome and lacks closely related paralogues in the genome (Prof. M. L. Chiusano, University "Federico II" of Naples, Italy, personal communication). By searching the PLACE database a number of pollen-specific activation elements AGAAA (Bate and Twell 1998) were identified (Fig. S2). These elements are also present in the promoter sequences of pollen-expressed *AtPMEI1*, *AtPMEI2* and *BoPMEI1* (Wolf et al. 2003; Zhang et al. 2010). In addition a number of CAAT and TATA tissue specific responsive elements present in genes expressed during fruit ripening (Atkinson et al. 1998; Yin et al. 2010) and a AWTTCAAA sequence, demonstrated to be responsive to ethylene (Montgomery et al. 1993) are also present.

The removal of the predicted N-terminal signal peptide generates a mature protein of 147 amino acids with a molecular mass of 16,129 Da and a predicted p$I = 7.74$ typical of cell wall bound proteins. Two potential N-glycosylation sites are present in the protein (Fig. S1); one of

them (Asn45) is also present in the TaPMEI sequence from wheat (Fig. 2). SolyPMEI shows the higher amino acid identity with AdPMEI (about 38 %) and with AtPMEI1 and AtPMEI2 (30 %) and exhibits four conserved cysteine residues typically engaged in the formation of two disulfide bridges that stabilize the α1 and α2 helices of the hairpin loop and the α4 and α5 helices of the four-helical bundle structure (Di Matteo et al. 2005). In addition, SolyPMEI has a conserved Thr-111 residue that strengthens the PMEI-PME interaction at the apoplastic pH, a typical SAA amino acid motif in α5 helix and a C-terminal hydrophobic region of six amino acids at the α6 helix involved in the stabilization of the four-helical bundle structure of the protein (Di Matteo et al. 2005). Like other PMEIs SolyPMEI lacks the Ala-83 residue insertion typical of INHs (Di Matteo et al. 2005) and the PKF motif that is critical for invertase-INH interaction (Hothorn et al. 2010) (Fig. 2).

The intronless region of SolyPMEI encoding the predicted mature protein was amplified by PCR using cDNA from tomato red fruit as a template. The amplified fragment was cloned and expressed in *Pichia pastoris*, which produced about 20 mg $l^{-1}$ of protein in the culture filtrate. SolyPMEI was purified to homogeneity and showed a single band with an apparent molecular mass, of 25 kDa by SDS-PAGE (Fig. 3a). The N-terminal sequencing led to the identification of 17 residues, EAEAEFDLIDEI-SKTD where the blank cycle at positions 13 is due to a Cys residue. The sequences EAEA and EF corresponded to the C-terminal of alpha factor signal peptide and the cloning vector restriction site respectively and DLIDEI-SKTD sequence corresponded to the N-terminal of SolyPMEI. The molecular mass of SolyPMEI, higher than expected, was also due to glycosylation as confirmed by the presence of two bands with a mass of 18 and 21 kDa, after treatment with endo-N-glycosidase, and corresponding to the fully

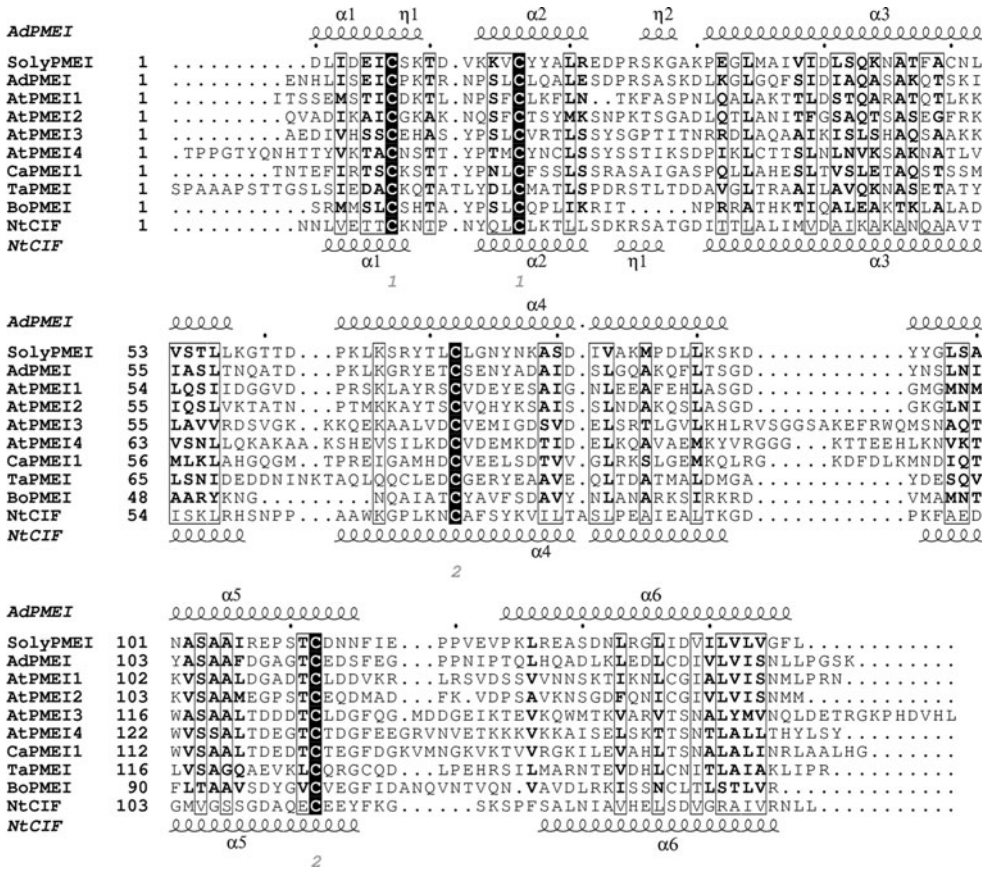


**Fig. 2** Amino acid sequence alignment of functionally characterized PMEI. The SolyPMEI amino acid sequence was aligned with PMEIs from Arabidopsis (AtPMEI1: At1g48020, AtPMEI2: At3g17220, AtPMEI3: At5g20740 and AtPMEI4: At4g25250), kiwi (AdPMEI: P83326), pepper (CaPMEI1: ABG47806), broccoli (BoPMEI: Q45TJ7) and wheat (TaPMEI: ACI01434). Tobacco cell wall invertase inhibitor (NtCIF: CAA73333) was also added for comparison. The alignment performed using ClustalW was manually adjusted according to PsiPred secondary structure predictions. Alignment was drawn by using the ESPript program. The secondary structure elements as elucidated in AdPMEI and NtCIF crystal structures are indicated at the *top* and at the *bottom* of the alignment, respectively. Invariant residues are *black shadowed* and similar residues are *boxed*. *Numbers 1* and *2* at the *bottom* denote disulfide bridges connecting the four conserved Cys residues

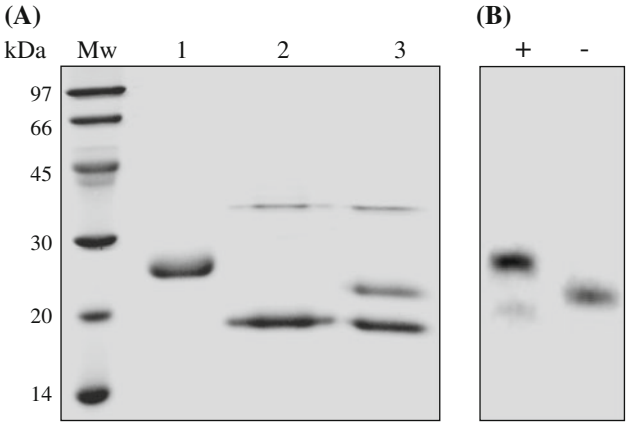


**Fig. 3** Heterologous expression and characterization of SolyPMEI. **a** Analysis of SolyPMEI glycosylation after endo N-glycosidase digestion: (*Mw*) molecular weight marker, (*1*) recombinant SolyPMEI, (*2*) SolyPMEI deglycosylated after denaturation, (*3*) SolyPMEI deglycosylated without previous denaturation. SDS-PGE gel performed under reducing conditions was stained with Comassie brilliant blue; **b** SDS-PAGE analysis and silver staining of SolyPMEI in reducing (+) and in non-reducing conditions (−)

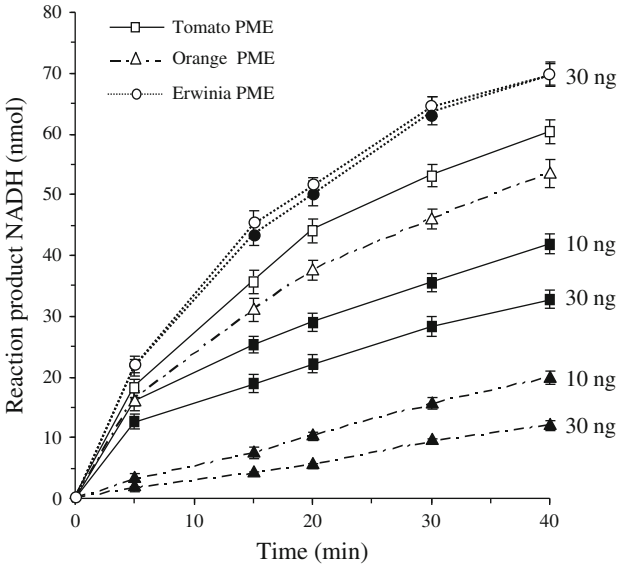


**Fig. 4** Inhibitory effect of SolyPMEI on plant and bacterial PMEs. PME activity from tomato crude extracts (*squares*), orange peel (*triangles*) or *E. chrysanthemi* (*circles*) are shown in the absence (*open symbols*) or in the presence (*closed symbols*) of SolyPMEI at the indicated amounts. *Bars* represent the average ± SD ($n = 3$)

and partially deglycosylated forms (Fig. 3a). The presence of intramolecular disulfide bridges was indicated by the higher SDS-PAGE mobility exhibited by the protein under non-reducing conditions as compared with the reduced form (Fig. 3b). The arrangement of the disulfide bridges between Cys7 and Cys16 and between Cys72 and Cys112 was determined by HPLC analysis as previously described (Camardella et al. 2000). The circular dichroism (CD) spectra of SolyPMEI and of the closely related AdPMEI were almost super-imposable in the range 240–195 nm and show two minima at 222 and 208 nm, typical of the α-helix structure, with a 68 % estimated content of α-helix (Fig. S3).

The inhibitory activity of SolyPMEI was assayed against microbial and plant PMEs. SolyPMEI inhibited both tomato and orange PMEs and was inactive against PME from *Erwinia chrysantemi* (Fig. 4) as well as against fruit specific tomato invertase (Reca et al. 2008).

In silico analysis predicts that SolyPMEI is targeted to the extracellular compartment (http://psort.hgc.jp/). In *N. benthamiana* leaves transiently expressing the *35S::SolyPMEI* gene SolyPMEI was immunodetected as a single band of 22 kDa in intercellular washing fluids (IWF) while it was not detected in intracellular protein fraction (Fig. 5a). G6PDH activity was not detected in IWF thus excluding cytosolic contaminations. PME activity measured in IWF extracted from *35S::SolyPMEI* was reduced of about 60 % respect to activity measured in IWF isolated from untransformed plants. No significant differences in PME activity was observed between IWF from leaves transformed with the empty pBI vector and untransformed controls.

The in vivo extracellular localization of SolyPMEI, as also reported for other characterized PMEI (Rockel et al. 2008; Zhang et al. 2010; Hong et al. 2010; Vandevenne et al. 2011; De Caroli et al. 2011), was demonstrated by the localization of GFP-SolyPMEI fusion protein in the extracellular space of transiently transformed Arabidopsis epidermal cells (Fig. 5b). All these results strongly indicate that SolyPMEI is secreted into the apoplast where acts as a functional inhibitor of PMEs.

## SolyPMEI is expressed in red fruit and interacts with PME-1

The expression of *SolyPMEI* in different tomato tissues was assessed by quantitative real-time PCR. The inhibitor was highly expressed in red fruits; in addition, *SolyPMEI* was expressed in flowers and pollen, albeit at a lower level (Fig. 6a). Different PMEI isoforms have been shown to be highly expressed in flowers and pollen (Raiola et al. 2004; Pina et al. 2005; Zhang et al. 2010). A role was demonstrated for PMEI in regulating the pollen tube growth and stability by locally inhibiting PME activity (Rockel et al. 2008; Zhang et al. 2010). Immunoblotting analysis confirmed the transcripts accumulation of the inhibitor in the different tissues (Fig. 6b). The expression of SolyPMEI in red fruits and the lack of expression in green fruits indicate a possible role of the inhibitor in the modulation of PME activity in ripening.

To identify the natural target of SolyPMEI in fruit, total proteins were separated from red fruits by gel-filtration

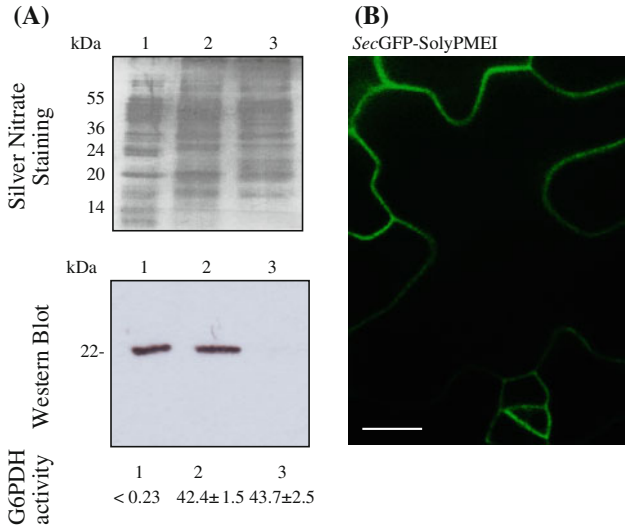


**Fig. 5** Apoplastic localization of SolyPME. **a** Immunoblot analysis was performed using purified antibodies against SolyPMEI on total protein extracted from tobacco leaves transiently transformed with *35S::SolyPMEI*, (1) proteins from intercellular washing fluids (IWF); (2) total proteins from leaf tissues; (3) total proteins from leaf tissues after IWF removal. Silver staining of proteins after SDS-PAGE separation is shown as loading control. Two µg of proteins were loaded for each fraction. G6PDH activity (nmol $min^{-1}$ $ml^{-1}$) was determined in the same fractions. The value 0.23 nmol $min^{-1}$ $ml^{-1}$ is the lowest G6PDH activity detectable in our samples. **b** Extracellular localization of *secGFP-SolyPMEI* transiently expressed in the epidermal cells of Arabidopsis leaves. *Scale bar* = 10 µm

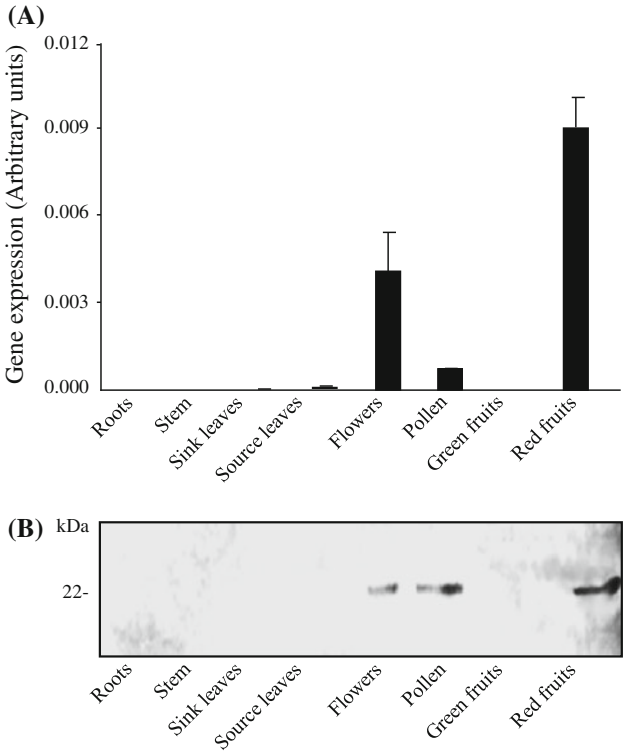


**Fig. 6** Analysis of SolyPMEI expression in tomato tissues. **a** Expression analysis of *SolyPMEI* in various tomato organs by real-time PCR. The relative level of gene expression was normalized with respect to *ACT4* mRNA. *Bars* represent the average ± SD ($n = 3$); **b** SDS-PAGE and immunoblot analysis of total protein extract (3 µg of proteins) from different tomato tissues performed using purified SolyPMEI antibodies

chromatography (Fig. 7a) and subjected to SDS-PAGE followed by immunoblot analysis. SolyPMEI expressed in *P. pastoris* used as a marker eluted in fraction 27 consistently with its molecular mass of 25 kDa (Fig. 7b). Instead, SolyPMEI from tomato pericarp, immunodetected as a band of 22 kDa, was present in the fractions 21–22, where proteins with an estimated molecular mass of about 45–60 kDa were eluted (Fig. 7a, c). No PME activity was associated to the presence of immunodetected bands. After SDS-PAGE separation and staining, proteins in fractions 21–22 were reduced, alkylated digested with trypsin, and analysed by LC–MS/MS and PME-1 (SwissProt accession P14280) the major isoenzyme present in tomato fruit (Markovic and Jörnvall 1986) was detected. Moreover, PME activity, consistently with the PMEs molecular mass of about 35 kDa, was present in fractions 25–26 where proteins with a molecular mass of about 30–40 kDa are eluted (Fig. 7a). These results indicate that SolyPMEI occurs as a complex with endogenous PME-1 and that active PME in free form was present in excess, whereas no PMEI in free form was detectable.

Tomato fruit proteins were also loaded onto an immunoaffinity *anti*SolyPMEI-Sepharose column. SDS-PAGE analysis of retained proteins showed the presence of two specific bands with an apparent molecular mass of 35 and 22 kDa (Fig. 7d). The N-terminal sequence of the 35 kDa protein band, by Edman degradation, identified a sequence of the tomato PME-1 isoform (IIANAVVAQD). N-terminal sequencing of the 22 kDa protein produced the DLI-DEI-S sequence of the mature SolyPMEI form where the blank cycle at position 7 is consistent with the presence of a Cys. The purification of the complex ruled out the masking of SolyPMEI to the antibodies by PME. The isolation of both SolyPMEI and PME-1 by gel-filtration chromatography and co-immunoprecipitation indicates that SolyPMEI is involved in the formation of a stable complex with the endogenous PME-1 isoform in tomato red fruits.

To further characterize the natural inhibitor, the SolyPMEI was also reduced, alkylated, digested with trypsin and analyzed by liquid chromatography-tandem mass spectrometry (LC–MS/MS). The identified fragments revealed an optimal matching with the deduced amino acid sequence and the coverage of 63 % of the entire sequence of the protein (Fig. S4). The sequence of the fragment 116–131 was detected only after deglycosylation of tryptic peptides, indicating that Asn101 is glycosylated in the fruit. On the other hand, the molecular mass of SolyPMEI is consistent

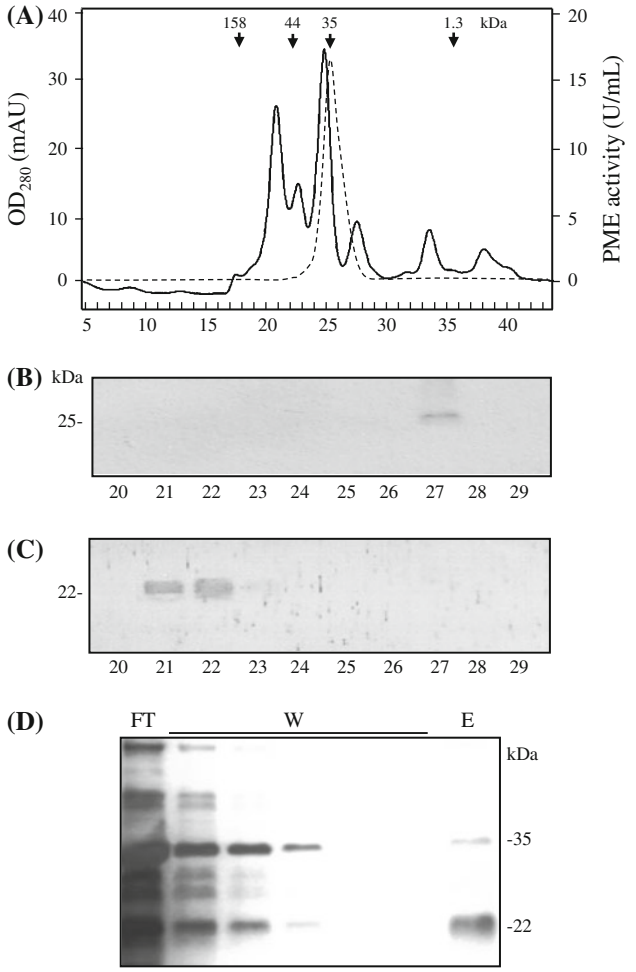


**Fig. 7** Identification of SolyPMEI in complex with its natural ligand. **a** Gel-filtration chromatogram of protein extracts from tomato red fruits (*solid line*) and PME activity (U x $mL^{-1}$) (*dashed line*). Gel filtration markers are indicated at the *top* of the figure; **b** Detection of purified SolyPMEI expressed in *P. pastoris* after gel filtration and SDS-PAGE followed by silver staining; **c** SDS-PAGE and immunoblot of natural SolyPMEI using antiSolyPMEI purified antibodies after gel filtration chromatography. The numbers of the eluted fractions are indicated at the *bottom* of the figures; **d** SDS-PAGE analysis and silver staining of proteins isolated after immunoaffinity chromatography. *FT* flow-through, *W* washing fractions, *E* fraction eluted from the affinity columns

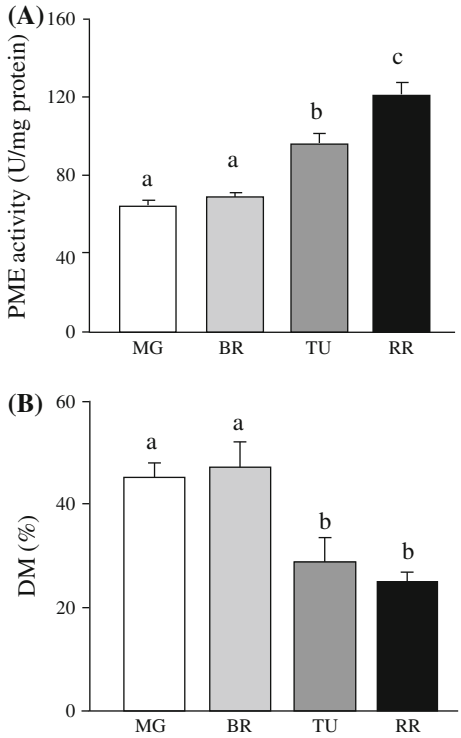


**Fig. 8** PME activity and degree of pectin methylesterification in tomato fruit at different stages of ripening. **a** PME activity from pericarp tissues at different stage of ripening i.e. 40 days (*mature green*, MG), 45 days (*breaker*, BR), 50 days (*turning*, TU) and 55 days (*red ripe*, RR) after anthesis; **b** degree of methylesterification of pericarp cell walls were quantified in tomato fruit at different stages of ripening. The *different letters* indicate data sets significantly different according to ANOVA followed by Tukey's test ($P < 0.01$). Data represent average ± SE ($n = 5$)

with the glycosylation of both predicted sites with a typical N-linked oligosaccharide of about 2.2 kDa as found in other plant secreted proteins (Ciardiello et al. 2008).

The glycosylation of SolyPMEI suggests that the inhibitor binds tomato PME-1 with a surface of interaction different from that of AdPMEI. In fact, in the model in which SolyPMEI replaces AdPMEI in the complex with tomato PME-1 (Di Matteo et al. 2005) (Fig. S5), the glycosylated Asn101 residue, substituting Tyr103 of AdPMEI, is located inside the contact interface between the inhibitor and the enzyme. The sterical hindrance of glycosidic moiety located at Asn101is predicted to prevent interaction between SolyPMEI and PME-1 by engaging the same surface as in the AdPMEI/PME-1 complex.

## SolyPMEI is expressed at specific stages of fruit ripening to modulate the spatial distribution of methylesterified pectins

The higher level of expression of SolyPMEI in red fruit as compared with the green fruit suggests the implication of the inhibitor in modulating the PME activity and degree of pectin esterification during ripening that it is expected to decrease from green to red ripe stages due to the accumulation of PME (Koch and Nevins 1989; Harriman et al. 1991). PME activity analysed in fruits at different stages of ripening was not significantly different at mature green (MG) and breaker (BR) stages and, as also reported by other authors (Tucker et al. 1982; Hall et al. 1994), significantly increased at turning (TU) and red ripe (RR) stages. An opposite trend was observed for the degree of methylesterification (Fig. 8a, b).

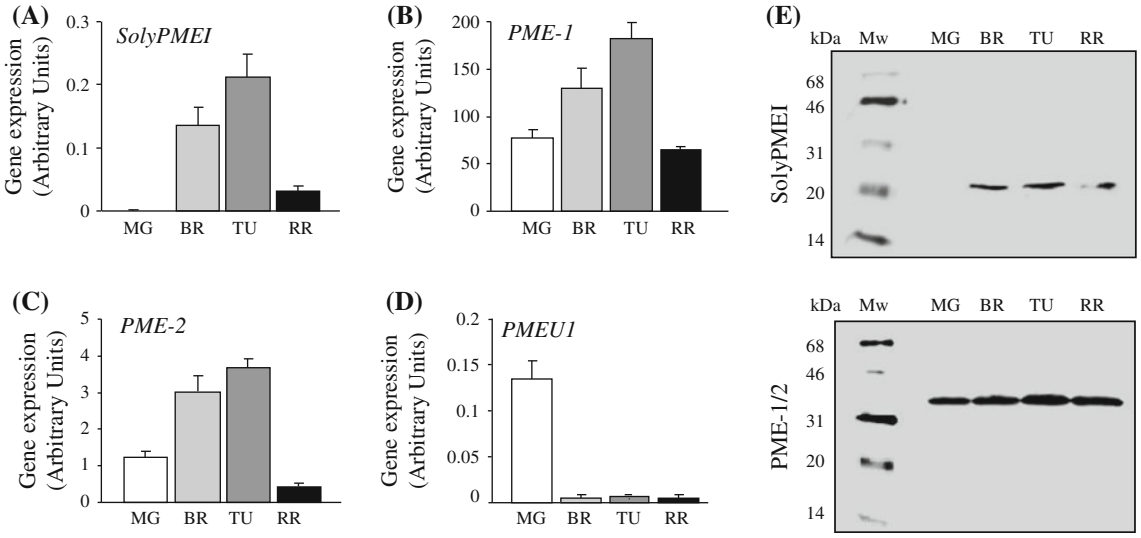


**Fig. 9** Analysis of the expression of *SolyPMEI* and specific PME isoforms in tomato fruits at different stages of ripening. Expression analysis of **a** *SolyPMEI*; **b** *PME-1*; **c** *PME-2;* **d** *PMEU1*; The transcript levels of different genes were revealed by quantitative RT-PCR. The relative level of gene expression was normalized with respect to *ACT4* mRNA. *Bars* represent the average ± SD ($n = 3$); **e** Western blot analysis of SolyPMEI and PME-1/2 in fruit at different stages of ripening by using antiSolyPMEI antibodies and monoclonal MA-TOM1-41B2 antibodies respectively. For SolyPMEI and PMEs immunodetection 10 and 3 µg of total proteins were loaded into the gel respectively

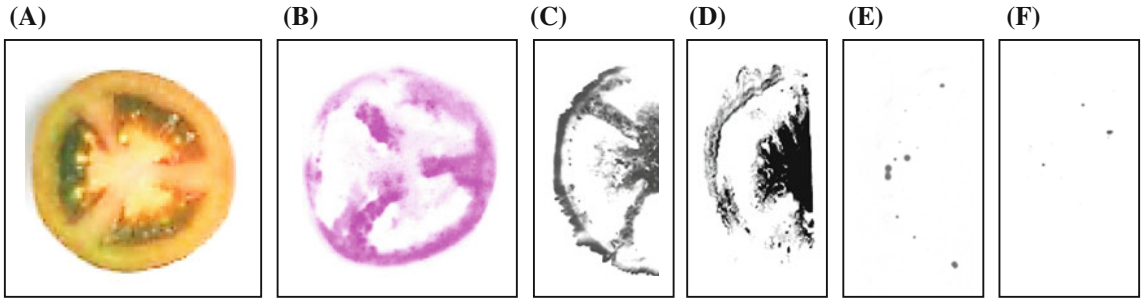


**Fig. 10** Tissue distribution of PME activity, SolyPMEI and methylesterified pectin in tomato fruit. **a** medially sliced tomato sections at turning stage of ripening used for tissue printing; **b** PME activity tissue-print. *Color* intensity indicates demethylesterification of pectin substrate; **c** Immunolocalization of SolyPMEI using antiSolyPMEI purified antibodies. **d** Immunolocalization of esterified pectins using LM20 monoclonal antibodies. Negative controls were performed using **e** rabbit or **f** rat secondary antibody alone. Each experiment was repeated five times with similar results

The expression of *SolyPMEI* analyzed by quantitative RT-PCR at different stages of ripening was compared with the expression of *PME-1* and *PME-2* that encode the major isoforms in ripe fruit (Pressey and Avants 1972; Tucker et al. 1982; Ray et al. 1988) and of *PMEU1*, the predominant isoform at early stages of fruit development (Phan et al. 2007). While no accumulation of *SolyPMEI* transcripts was detected at MG stage, the expression of the inhibitor increased at BR stage, reached a maximum at TU stage and declined at RR stage (Fig. 9a). Concomitant with the increase of *SolyPMEI* the *PME-1* and *PME-2* transcripts also increased at BR and TU stages and declined at RR stages (Fig. 9b, c).

To explain the increase of PME activity at RR stage with respect TU stage despite the relative decrease of *PME-1* and *PME-2* expression level, the accumulation of PMEs and SolyPMEI was studied by immunoblot analysis with anti SolyPMEI antibodies and MA-TOM1-41B2 antibodies recognizing both PME-1 and PME-2 isoforms (Vandevenne et al. 2009). Immunoblotting analysis showed that the inhibitor is absent at MG stage, mainly accumulates at BR and TU stages and declines at RR stages consistently with the transcripts analysis (Fig. 9a, e) while PME-1/2 level slightly increase up to TU stage and remains quite constant at RR stage of ripening (Fig. 9e). The increase of PME activity at RR stage with respect to TU stage is, therefore, likely due to the concomitant decrease of the inhibitor at the latter stage of ripening.

Conversely, the specific expression of *PMEU1* at MG stage (Fig. 9d) indicates that its contribution is not relevant

to the total PME activity in ripe fruit and makes this isoform an unlikely target of the inhibitor in the fruit.

Our results strongly suggest that SolyPMEI regulates PME activity during ripening mainly at BR, TU and RR stages. Consistently the increase of PMEI expression level with progression of ripening was also observed in kiwi (Irifune et al. 2004) where the inhibitor, undetectable in unripe fruit, is only found in mature fruit (Camardella et al. 2000).

The in situ localization of PME activity, SolyPMEI and pectin structure was performed to elucidate the possible functional role of SolyPMEI in pectin metabolism. The tissue spatial distribution of PME activity in mature fruit showed high PME activity dispersed throughout the pericarp and a relative lower activity in the columella (Fig. 10b). The spatial co-localization of SolyPMEI and highly methylesterified pectin in the columella (Fig. 10c, d) suggested that SolyPMEI regulates the zonal pattern of esterified pectin in the fruit tissue.

## Conclusion

PMEs show a large number of isoforms in plants that reflect their multiple roles in the modification of cell wall during growth and development. PMEIs are thought to provide an efficient post-transcriptional control mechanism of PME activity *in planta*. In this work we have identified a tomato PMEI that typically inhibit plant PMEs and demonstrated its in vivo localization in the same compartment where PMEs are inhibited. SolyPMEI is expressed in flower, pollen and fruit. The occurrence of transcripts in flower and pollen suggests a developmental role of this inhibitor during flower formation and reproductive processes that remains to be investigated.

PME activity is known to be involved in tissue integrity, texture and softening in fruit ripening (Tucker et al. 1982; Harriman et al. 1991; Blumer et al. 2000; Brummell and Harpster 2001) and our results provide evidence of the possible physiological role of PMEI in regulating PME activity during this process. In ripe fruit SolyPMEI is engaged in the formation of an inactive complex with the prevalent PME-1 isoform and both proteins are co-expressed at specific stages of ripening in tomato fruit. We have also studied the expression of SolyPMEI and PME isoforms during fruit ripening in relation with the PME activity and degree of pectin esterification. The analysis of the zonal distribution of PME activity and the in situ co-localization of SolyPMEI with high esterified pectins suggest that SolyPMEI regulates the spatial patterning of distribution of esterified pectins in fruit. PMEI likely maintains a high methylesterification status of pectin to limit/prevent the local degradation by fruit specific pectinases that affect the tissue firmness.

**Acknowledgments** We would like to thank Prof. J. P. Knox for providing LM20 antibodies and Prof. M. E. Hendrickx for MATOM1-41B2 antibodies. This work was supported by the European Research Council (ERC Advanced Grant No. 233083), grant (C26A09RCP9) by "Sapienza" University of Rome, and by the Italian Ministry of Foreign Affairs.

## References

An SH, Sohn KH, Choi HW, Hwang IS, Lee SC, Hwang BK (2008) Pepper pectin methylesterase inhibitor protein CaPMEI1 is required for antifungal activity, basal disease resistance and abiotic stress tolerance. Planta 228:61–78

Atkinson RG, Bolitho KM, Wright MA, Iturriagagoitia-Bueno T, Reid SJ, Ross GS (1998) Apple ACC-oxidase and polygalacturonase: ripening-specific gene expression and promoter analysis in transgenic tomato. Plant Mol Biol 38:449–460

Balestrieri C, Castaldo D, Giovane A, Quagliuolo L, Servillo L (1990) A glycoprotein inhibitor of pectin methylesterase in kiwi fruit (*Actinidia chinensis*). Eur J Biochem 193:183–187

Bate N, Twell D (1998) Functional architecture of a late pollen promoter: pollen-specific transcription is developmentally regulated by multiple stage-specific and co-dependent activator elements. Plant Mol Biol 37:859–869

Blumer JM, Clay RP, Bergmann CW, Albersheim P, Darvill A (2000) Characterization of changes in pectin methylesterase expression and pectin esterification during tomato fruit ripening. Can J Bot 78:607–618

Bordenave M, Goldberg R (1993) Purification and characterization of pectin methylesterases from Mung bean hypocotyl cell walls. Phytochemistry 33:999–1003

Bosch M, Cheung AY, Hepler PK (2005) Pectin methylesterase, a regulator of pollen tube growth. Plant Physiol 138:1334–1346

Brummell DA, Harpster MH (2001) Cell wall metabolism in fruit softening and quality and its manipulation in transgenic plants. Plant Mol Biol 47:311–340

Camardella L, Carratore V, Ciardiello MA, Servillo L, Balestrieri C, Giovane A (2000) Kiwi protein inhibitor of pectin methylesterase amino-acid sequence and structural importance of two disulfide bridges. Eur J Biochem 267:4561–4565

Cervone F, De Lorenzo G, Degrà L, Salvi G, Bergami M (1987) Purification and characterization of a polygalacturonase- inhibiting protein from *Phaseolus vulgaris* L. Plant Physiol 85:631–637

Chen M-H, Citovsky V (2003) Systemic movement of a tobamovirus requires host cell pectin methylesterase. Plant J 35:386–392

Ciardiello MA, D'Avino R, Amoresano A, Tuppo L, Carpentieri A, Carratore V, Tamburrini M, Giovane A, Pucci P, Camardella L (2008) The peculiar structural features of kiwi fruit pectin methylesterase: Amino acid sequence, oligosaccharides structure, and modeling of the interaction with its natural proteinaceous inhibitor. Proteins 71:195–206

De Caroli M, Lenucci MS, Di Sansebastiano GP, Dalessandro G, De Lorenzo G, Piro G (2011) Protein trafficking to the cell wall occurs through mechanisms distinguishable from default sorting in tobacco. Plant Journal 65:295–308

Di Matteo A, Giovane A, Raiola A, Camardella L, Bonivento D, De Lorenzo G, Cervone F, Bellincampi D, Tsernoglou D (2005) Structural basis for the interaction between pectin methylesterase and a specific inhibitor protein. Plant Cell 17:849–858

Di Sansebastiano GP, Paris N, Marc-Martin S, Neuhaus JM (1998) Specific accumulation of GFP in a non-acidic vacuolar compartment via a C-terminal propeptide-mediated sorting pathway. Plant Journal 15:449–457

Dorokhov YL, Makinen K, Frolova OY, Merits A, Saarinen J, Kalkkinen N, Atabekov JG, Saarma M (1999) A novel function for a ubiquitous plant enzyme pectin methylesterase: the host-cell receptor for the tobacco mosaic virus movement protein. FEBS Lett 461:223–228

Felsenstein J (1985) Confidence limits on phylogenies: an approach using the bootstrap. Evolution 39:783–791

Ferrari S, Galletti R, Pontiggia D, Manfredini C, Lionetti V, Bellincampi D, Cervone F, De Lorenzo G (2008) Transgenic expression of a fungal endo-polygalacturonase increases plant resistance to pathogens and reduces auxin sensitivity. Plant Physiol 146:669–681

Futamura N, Mori H, Kouchi H, Shinohara K (2000) Male flower-specific expression of genes for polygalacturonase, pectin methylesterase and beta-1,3-glucanase in a dioecious willow (*Salix gilgiana* Seemen). Plant Cell Physiol 41:16–26

Gaffe J, Tiznado ME, Handa AK (1997) Characterization and functional expression of a ubiquitously expressed tomato pectin methylesterase. Plant Physiol 114:1547–1556

Giovane A, Balestrieri C, Quagliuolo L, Castaldo D, Servillo L (1995) A glycoprotein inhibitor of pectin methylesterase in kiwi fruit - Purification by affinity chromatography and evidence of a ripening-related precursor. Eur J Biochem 233:926–929

Greer J (1990) Comparative modeling of proteins in the design of novel renin inhibitors. Biophys J 57:A207

Grsic-Rausch S, Rausch T (2004) A coupled spectrophotometric enzyme assay for the determination of pectin methylesterase activity and its inhibition by proteinaceous inhibitors. Anal Biochem 333:14–18

Hall TA (1999) BioEdit: a user-friendly biological sequence alignment editor and analysis program for Windows 95/98/NT. Nucleic Acids Symp Ser 41:95–98

Hall LN, Bird CR, Picton S, Tucker GA, Seymour GB, Grierson D (1994) Molecular characterization of cDNA clones representing pectin esterase isozymes from tomato. Plant Mol Biol 25:313–318

Hao YL, Huang XY, Mei XH, Li RY, Zhai ZY, Yin S, Huang Y, Luo YB (2008) Expression, purification and characterization of pectin methylesterase inhibitor from kiwi fruit in *Escherichia coli*. Protein Expr Purif 60:221–224

Harriman RW, Tieman DM, Handa AK (1991) Molecular cloning of tomato pectin methylesterase gene and its expression in Rutgers, ripening inhibitor, nonripening, and never ripe tomato fruits. Plant Physiol 97:80–87

Haseloff J, Siemering KR, Prasher DC, Hodge S (1997) Removal of a cryptic intron and subcellular localization of green fluorescent protein are required to mark transgenic *Arabidopsis* plants brightly. Proc Natl Acad Sci USA 94:2122–2127

Hasunuma T, Fukusaki E, Kobayashi A (2004) Expression of fungal pectin methylesterase in transgenic tobacco leads to alteration in cell wall metabolism and a dwarf phenotype. J Biotechnol 111:241–251

Hewezi T, Howe P, Maier TR, Hussey RS, Mitchum MG, Davis EL, Baum TJ (2008) Cellulose binding protein from the parasitic nematode *Heterodera schachtii* interacts with arabidopsis pectin methylesterase: cooperative cell wall modification during parasitism. Plant Cell 20:3080–3093

Hong MJ, Kim DJ, Lee TG, Jeon WB, Seo YW (2010) Functional characterization of pectin methylesterase inhibitor (PMEI) in wheat. Genes Genet Syst 85:97–106

Hothorn M, Van den Ende W, Lammens W, Rybin V, Scheffzek K (2010) Structural insights into the pH-controlled targeting of plant cell-wall invertase by a specific inhibitor protein. Proc Nat Acad Sci USA 107:17427–17432

Irifune K, Nishida T, Egawa H, Nagatani A (2004) Pectin methylesterase inhibitor cDNA from kiwi fruit. Plant Cell Rep 22:333–338

Jolie RP, Duvetter T, Van Loey AM, Hendrickx ME (2010) Pectin methylesterase and its proteinaceous inhibitor: a review. Carbohydr Res 345:2583–2595

Juge N (2006) Plant protein inhibitors of cell wall degrading enzymes. Trends Plant Sci 11:359–367

Koch JL, Nevins DJ (1989) Tomato fruit cell wall. I. Use of purified tomato polygalacturonase and pectinmethylesterase to identify developmental changes in pectins. Plant Physiol 91:816–822

Kojima K, Sakurai N, Kuraishi S, Yamamoto R, Nevins DJ (1991) Novel technique for measuring tissue firmness within tomato (Lycopersicon-Esculentum Mill) fruit. Plant Physiol 96:545–550

Limberg G, Korner R, Buchholt HC, Christensen TM, Roepstorff P, Mikkelsen JD (2000) Analysis of different de-esterification mechanisms for pectin by enzymatic fingerprinting using endopectin lyase and endopolygalacturonase II from *A. niger*. Carbohydr Res 327:293–307

Lionetti V, Raiola A, Camardella L, Giovane A, Obel N, Pauly M, Favaron F, Cervone F, Bellincampi D (2007) Overexpression of pectin methylesterase inhibitors in Arabidopsis restricts fungal infection by *Botrytis cinerea*. Plant Physiol 143:1871–1880

Lionetti V, Francocci F, Ferrari S, Volpi C, Bellincampi D, Galletti R, D'Ovidio R, De Lorenzo G, Cervone F (2010) Engineering the cell wall by reducing de-methyl-esterified homogalacturonan improves saccharification of plant tissues for bioconversion. Proc Natl Acad Sci USA 107:616–621

Lohaus G, Pennewiss K, Sattelmacher B, Hussmann M, Hermann MK (2001) Is the infiltration-centrifugation technique appropriate for the isolation of apoplastic fluid? A critical evaluation with different plant species. Physiol Plant 111:457–465

Markovic O, Janecek S (2001) Pectin degrading glycoside hydrolases of family 28: sequence-structural features, specificities and evolution. Protein Eng 14:615–631

Markovic O, Janecek S (2004) Pectin methylesterases: sequence-structural features and phylogenetic relationships. Carbohydr Res 339:2281–2295

Markovic O, Jörnvall H (1986) Pectinesterase - the Primary Structure of the Tomato Enzyme. Eur J Biochem 158:455–462

Matsudaira P (1987) Sequence from picomole quantities of proteins electroblotted onto polyvinylidene difluoride membranes. J Biol Chem 262:10035–10038

McCartney L, Ormerod AP, Gidley MJ, Knox JP (2000) Temporal and spatial regulation of pectic (1-4)-beta-D-galactan in cell walls of developing pea cotyledons: implications for mechanical properties. Plant J 22:105–113

Mei XH, Hao YL, Zhu HL, Gao HY, Luo YB (2007) Cloning of pectin methylesterase inhibitor from kiwi fruit and its high expression in *Pichia pastoris*. Enzyme Microbial Technol 40:1001–1005

Mohnen D (2008) Pectin structure and biosynthesis. Curr Op Plant Biol 11:266–277

Montgomery J, Goldman S, Deikman J, Margossian L, Fischer RL (1993) Identification of an ethylene-responsive region in the promoter of a fruit ripening gene. Proc Natl Acad Sci USA 90:5939–5943

Orfila C, Huisman MM, Willats WG, van Alebeek GJ, Schols HA, Seymour GB, Knox JP (2002) Altered cell wall disassembly during ripening of Cnr tomato fruit: implications for cell adhesion and fruit softening. Planta 215:440–447

Peaucelle A, Louvet R, Johansen JN, Hofte H, Laufs P, Pelloux J, Mouille G (2008) Arabidopsis phyllotaxis is controlled by the methyl-esterification status of cell-wall pectins. Curr Biol 18: 1943–1948

Pelletier S, Van Orden J, Wolf S, Vissenberg K, Delacourt J, Ndong YA, Pelloux J, Bischoff V, Urbain A, Mouille G, Lemonnier G, Renou JP, Hofte H (2010) A role for pectin de-methylesterification in a developmentally regulated growth acceleration in dark-grown Arabidopsis hypocotyls. New Phytol 188:726–739

Pelloux J, Rusterucci C, Mellerowicz EJ (2007) New insights into pectin methylesterase structure and function. Trends Plant Sci 12:267–277

Pfaffl MW (2001) A new mathematical model for relative quantification in real-time RT-PCR. Nucleic Acids Res 29:e45

Phan TD, Bo W, West G, Lycett GW, Tucker GA (2007) Silencing of the major salt-dependent isoform of pectinesterase in tomato alters fruit softening. Plant Physiol 144:1960–1967

Pilling J, Willmitzer L, Bucking H, Fisahn J (2004) Inhibition of a ubiquitously expressed pectin methyl esterase in *Solanum tuberosum* L. affects plant growth, leaf growth polarity, and ion partitioning. Planta 219:32–40

Pina C, Pinto F, Feijo JA, Becker JD (2005) Gene family analysis of the Arabidopsis pollen transcriptome reveals biological implications for cell growth, division control, and gene expression regulation. Plant Physiol 138:744–756

Prasanna V, Prabha TN, Tharanathan RN (2007) Fruit ripening phenomena—an overview. Crit Rev Food Sci Nutr 47:1–19

Pressey R, Avants JK (1972) Multiple forms of pectinesterase in tomatoes. Phytochemistry 11:3139–3142

Raiola A, Camardella L, Giovane A, Mattei B, De Lorenzo G, Cervone F, Bellincampi D (2004) Two *Arabidopsis thaliana* genes encode functional pectin methylesterase inhibitors. FEBS Lett 557:199–203

Raiola A, Lionetti V, Elmaghraby I, Immerzeel P, Mellerowicz EJ, Salvi G, Cervone F, Bellincampi D (2011) Pectin methylesterase is induced in Arabidopsis upon infection and is necessary for a successful colonization by necrotrophic pathogens. Mol Plant-Microbe Interact 24:432–440

Ray J, Knapp J, Grierson D, Bird C, Schuch W (1988) Identification and sequence determination of a cDNA clone for tomato pectin esterase. Eur J Biochem 174:119–124

Reca IB, Brutus A, D'Avino R, Villard C, Bellincampi D, Giardina T (2008) Molecular cloning, expression and characterization of a novel apoplastic invertase inhibitor from tomato (*Solanum lycopersicum*) and its use to purify a vacuolar invertase. Biochimie 90:1611–1623

Ren C, Kermode AR (2000) An increase in pectin methyl esterase activity accompanies dormancy breakage and germination of yellow cedar seeds. Plant Physiol 124:231–242

Rockel N, Wolf S, Kost B, Rausch T, Greiner S (2008) Elaborate spatial patterning of cell-wall PME and PMEI at the pollen tube tip involves PMEI endocytosis, and reflects the distribution of esterified and de-esterified pectins. Plant J 53:133–143

Saitou N, Nei M (1987) The neighbor-joining method: a new method for reconstructing phylogenetic trees. Mol Biol Evol 4:406–425

Sali A, Blundell TL (1993) Comparative protein modeling by satisfaction of spatial restraints. J Mol Biol 234:779–815

Scognamiglio MA, Ciardiello MA, Tamburrini M, Carratore V, Rausch T, Camardella L (2003) The plant invertase inhibitor shares structural properties and disulfide bridges arrangement with the pectin methylesterase inhibitor. J Prot Chem 22:363–369

Shevchenko A, Wilm M, Vorm O, Mann M (1996) Mass spectrometric sequencing of proteins from silver stained polyacrylamide gels. Anal Chem 68:850–858

Sicilia F, Mattei B, Cervone F, Bellincampi D, De Lorenzo G (2005) Characterization of a membrane-associated apoplastic lipoxygenase in *Phaseolus vulgaris* L. Biochim Biophys Acta 1748:9–19

Steele NM, McCann MC, Roberts K (1997) Pectin modification in cell walls of ripening tomatoes occurs in distinct domains. Plant Physiol 114:373–381

Tamura K, Dudley J, Nei M, Kumar S (2007) MEGA4: molecular evolutionary genetics analysis (MEGA) software version 4.0. Mol Biol Evol 24:1596–1599

Tieman DM, Harriman RW, Ramamohan G, Handa AK (1992) An antisense pectin methylesterase gene alters pectin chemistry and soluble solids in tomato fruit. Plant Cell 4:667–679

Tucker GA, Robertson NG, Grierson D (1982) Purification and changes in activities of tomato pectinesterase isoenzymes. J Sci Fd Agric 33:396–400

Vandevenne E, Van Buggenhout S, Duvetter T, Brouwers E, Declerck PJ, Hendrickx ME, Van Loey A, Gils A (2009) Development and evaluation of monoclonal antibodies as probes to assess the differences between two tomato pectin methylesterase isoenzymes. J Immunol Meth 349:18–27

Vandevenne E, Christiaens S, Van Buggenhout S, Jolie RP, Gonzalez-Vallinas M, Duvetter T, Declerck PJ, Hendrickx ME, Gils A, Van Loey A (2011) Advances in understanding pectin methylesterase inhibitor in kiwi fruit: an immunological approach. Planta 233:287–298

Verhertbruggen Y, Marcus SE, Haeger A, Ordaz-Ortiz JJ, Knox JP (2009) An extended set of monoclonal antibodies to pectic homogalacturonan. Carbohydr Res 344:1858–1862

Volpi C, Janni M, Lionetti V, Bellincampi D, Favaron F, D'Ovidio R (2011) The ectopic expression of a pectin methyl esterase inhibitor increases pectin methyl esterification and limits fungal diseases in wheat. Mol Plant-Microbe Interact 24:1012–1019

Wakabayashi K, Hoson T, Huber DJ (2003) Methyl de-esterification as a major factor regulating the extent of pectin depolymerization during fruit ripening: a comparison of the action of avocado (*Persea americana*) and tomato (*Lycopersicon esculentum*) polygalacturonases. J Plant Physiol 160:667–673

Wakeley PR, Rogers HJ, Rozycka M, Greenland AJ, Hussey PJ (1998) A maize pectin methylesterase-like gene, ZmC5, specifically expressed in pollen. Plant Mol Biol 37:187–192

Wolf S, Grsic-Rausch S, Rausch T, Greiner S (2003) Identification of pollen-expressed pectin methylesterase inhibitors in Arabidopsis. FEBS Lett 555:551–555

Wolf S, Mouille G, Pelloux J (2009) Homogalacturonan methyl-esterification and plant development. Mol Plant 2:851–860

Yin XR, Allan AC, Chen KS, Ferguson IB (2010) Kiwifruit EIL and ERF Genes Involved in Regulating Fruit Ripening. Plant Physiol 153:1280–1292

Zhang GY, Feng J, Wu J, Wang XW (2010) BoPMEI1, a pollen-specific pectin methylesterase inhibitor, has an essential role in pollen tube growth. Planta 231:1323–1334